Published in: Atlas of Visualization, Vol III, FlowVis. Soc. Japan eds., CRC Press, (1997), pp 99-113.

chapter six

Flow Visualization in Turbulent Large-Scale Structure Research

Lorenz W. Sigurdson

Mechanical Engineering Department, University of Alberta, Edmonton, AB, Canada

Abstract—*Examples are given of how flow visualization has been used to discover the large-scale coherent structures in four different turbulent flow types. These are the separated and reattaching flows over a blunt-faced circular cylinder aligned coaxially with the free stream and its two-dimensional analog the blunt flat plate; the vortex ring resulting from a nuclear explosion; a water drop impacting on a pool of water; and a bursting air bubble initially resting on a free surface. A brief review is given of the general methodology used for interpretation of data obtained by direct injection of tracer materials. Each flow is discussed in terms of the visualization technique used and what conclusions about the structure and other flow aspects could be deduced. The topological similarity between the three-dimensional and unsteady vortex structures of these four flow types is stressed.*

Introduction

Vorticity, a local "spinning" of a fluid, is present in most fluid flows. The more well-known cases of vorticity creation are as follows. It can be created at the solid physical boundaries of a fluid where a pressure gradient is present, for example, the hood of an automobile. It is created within the fluid where there are components of gradients in density perpendicular to the local pressure gradient, for example, a buoyant thermal which keeps a sailplane aloft. Fluid–fluid interfaces can also give birth to vorticity. Where the vorticity goes from there influences many things of engineering importance such as: lift and drag on an aircraft wing, wind forces on buildings, noise production from turbulence, and valve closure within the human heart.

Research suggests that vorticity does not disperse completely randomly but often forms organized large-scale structures, as discussed by Roshko (1976). Within the apparent chaos, an orderly identifiable large-scale structure often exists. These structures are essentially regions of vorticity. Saffman (1980) stated that it is now proposed that turbulence be modeled as the creation, evolution, interaction, and decay of these structures. In his book (Saffman, 1992), he continues:

> The discovery of coherent structures in turbulence has fostered the hope that the study of vortices will lead to models and an understanding of turbulent flow, thereby solving or at least making less mysterious one of the great unsolved problems of classical physics.

0-8493-2657-8/97/$0.00+$.50

Knowledge of the flow structure offers new potential to control turbulent flows to the engineer's advantage. This could be done using steady or unsteady and/or spatially varying forcing techniques such as sound or moving control surfaces. This could result in drag reduction on automobiles and aircraft, improved combustion efficiency, and improved efficiency of an array of mechanical devices.

It is supposed that each particular flow geometry will have a characteristic vortical structure. Its determination is not unlike the task in chemistry of determining the structure of a molecule once the constituent elements are known. Much can be surmised with a few bits of knowledge about the expected behavior of the flow, and an understanding of what the location of the vorticity means to things like conservation of momentum and the velocity field (from the Biot-Savart law). Neglecting viscous diffusion, the vorticity moves as a material element with the flow; therefore, many simple vortex interactions can be deduced by knowing the velocity field the vorticity would induce.

Flow visualization has proven to be a very useful tool for determining the nature of the large-scale structure for any particular flow geometry. It is one of the most straightforward methods of obtaining *field* measurements of the vortex trajectories. Previous stigma associated with doing flow visualization (due to its perceived qualitative nature) and a reliance on time-averaged measurements at individual *points* actually hindered the turbulence research community's realization of the existence of large-scale structures. If the tracer is somehow placed in the cores of the vortices of interest early on in their evolution, then their motion due to convection can be observed.

There has been, since Roshko's (1976) paper, an explosion of work in the area of elucidating large-scale structures in turbulence, particularly the free shear layer problem. This paper will give some examples of how visualization has been used to discover the structure in a limited subset of this research: separated flows, an above-ground nuclear test, water drops impacting on a pool of still water, and bursting air bubbles initially resting on such a pool. Each flow will be discussed briefly in terms of the visualization technique used and an overview of what conclusions about the structure as well as other flow aspects could be drawn from the results. Rather than a comprehensive review of the research done for each flow (for example, for the separation bubble there has been quite a lot as is reviewed in Sigurdson, 1995), we will chronicle the efforts of one research program designed to elucidate the interconnectedness of the large-scale structure between these particular flows.

There is a surprising similarity between the structures that is the focus of the program. These similarities will not be discussed in detail here, other than to explain the contribution of the flow visualization. The similarities will be part of other papers to follow. In an extension of the chemistry analogy suggested earlier, the study of large-scale structures in turbulence is, relatively, only slightly more advanced than the fuzzy understanding of the constituents of matter in Dimitri Mendeleyev's time. Yet Mendeleyev, in 1869, was able to construct a periodic table which predicted possible chemical reactions and the existence of previously unknown elements. Perhaps it will be possible to organize the turbulent flow structures in a "periodic table" in a similar way to Mendeleyev, which may help improve the overall understanding and possibly predict the existence of unknown flow behaviors.

General Methodology

Two main techniques of visualization will be discussed in the following sections: in air, direct smoke injection via probe or smoke-wire, and in liquids, direct injection of dye, either colored or fluorescent. Illumination is primarily from tungsten or strobe lamps for the former, and fluorescent tube banks, strobe or argon-ion laser for the latter. Data acquisition is mainly through a 35-mm camera, however, a 16-mm movie camera and a

standard video camera running with continuous illumination for slow flows or synchronized to a strobe for faster flows have also been used to provide sequential information. The video camera synchronized to the strobe is especially useful for immediate feedback on the fine tuning of the experiment. If expense is not a consideration, there are, of course, constantly improving means of electronic image capture, not discussed here. Other than the use of the laser, the techniques used here are not particularly sophisticated, yet we shall see that for the first observation of a flow they can be very informative.

The general methodology in each case is to ensure that some tracer (dye or smoke) is injected at or passes through the region of vorticity creation, or due to the nature of the flow becomes associated with or entrained into the vorticity-bearing parts of the flow. Freymuth (1966) notes that in a two-dimensional inviscid fluid flow, due to the Helmholtz equation, the vorticity is convected in the same way as a material element of the fluid. The concept can be extended to three-dimensional inviscid flow by the application of Helmholtz's laws of vortex motion of 1858. These state that for an ideal barotropic fluid under the action of conservative external body forces, vortex lines move with the fluid (Saffman, 1992). Therefore, if tracer is applied to the fluid material elements that are vortical, the tracer will follow the path of the vorticity. There is not, however, a linear relationship between the *concentration* of dye and the *magnitude* of the vorticity, only a one-to-one relationship between the locations. For instance, vorticity magnitude is increased when stretched, whereas the dye concentration will weaken. This is discussed by Kida and Takaoka (1994).

Complications can also arise due to the fact that fluids are not, in general, inviscid. This means that the Schmidt number (Sc) becomes important, which represents the ratio of the diffusion rate of the vorticity due to viscosity to the rate of diffusion of the tracer. ($Sc = \nu/k, \nu$ = kinematic viscosity, k = diffusivity of tracer.) As an example, for dye in water the vorticity diffuses faster than the dye, therefore the absence of dye in some location does not guarantee the absence of vorticity there; the vorticity may have diffused to that place while the tracer hasn't. However, if the dye is initially placed with the vorticity, the locations of the dye can still be inferred to be the positions of highest vortical intensity. If the Reynolds number (Re) of the flow is high (indicative of the ratio of inertial forces to viscous forces, $Re = \rho UL/\mu$, ρ = density of fluid, U = characteristic velocity, L = characteristic length, and μ = absolute viscosity), then the convection of the vorticity is more important than the diffusion and the location of tracer becomes more closely associated to the location of vorticity.

Another caution to be heeded is that the tracer does not become canceled in the presence of other tracer which identifies vorticity of opposite sign, whereas it is possible that the vorticity could. Also, if the tracer is *not* initially placed with the vorticity, very careful interpretation of the results must be exercised.

Cimbala et al. (1988) comment on another danger. They studied the streaklines emanating from a smoke-wire which were introduced upstream of the Kármán vortex street behind a circular cylinder at moderately low Reynolds numbers. Previous interpretations indicated vortices, when in actuality the wake had relaminarized. This alerted researchers to the difficulties involved in streakline interpretation and the importance of introducing the tracer near the part of the flow that was of interest. The streaklines represent an integration of all that has happened to the tracer particles from the points of introduction, and *not* only what has happened in the instants before the photograph is taken.

Specific Examples

The Blunt Cylinder and the Blunt Flat Plate

A characteristic three-dimensional, unsteady vortex structure has been proposed for the flow in the reattachment region of a separation bubble (Sigurdson and Roshko, 1984;

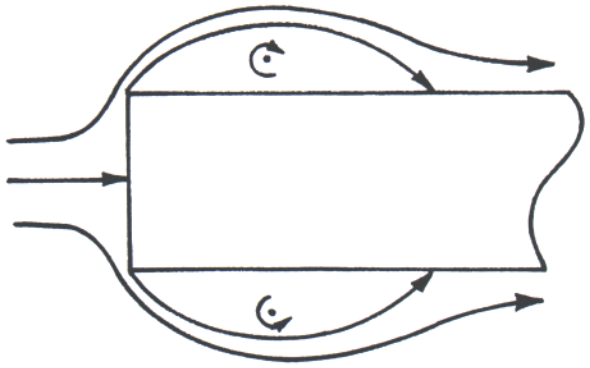

Figure 1 Profile view of the cylinder or plate showing time-averaged streamlines.

Sigurdson, 1986). The bubble was located downstream of the sharp-edged blunt face of a circular cylinder aligned coaxially with the free stream. Another bubble was also studied, the one associated with the two-dimensional analog of this body shape, the sharp-edged blunt flat plate. The same qualitative vortex structure was found to occur there. Figure 1 is a diagram showing the profile view of the cylinder or plate and the time-averaged separating and reattaching streamline that borders the recirculation region.

Flow visualization also played an important role in determining the influence of periodic velocity perturbations on the circular cylinder flow (Sigurdson, 1995; Sigurdson, 1986; Sigurdson et al., 1981). This research was initiated to determine whether the flow could be influenced in a beneficial way, for instance, to reduce the drag on the cylinder. Acoustically generated velocity perturbations were introduced to the flow through a small circumferential gap located immediately downstream of the fixed separation line at the sharp shoulder of the cylinder face. Time-averaged pressure measurements indicated that the drag was reduced. The task then came to explain why and to find what frequencies and amplitudes of excitation created the optimum results.

Smoke was injected into the flow using two methods, from a probe upstream of the model and from a smoke-wire. The smoke-wire is a wire which has had oil dripped down it that beads up into discrete accumulations. When current is passed through the wire it heats up and smoke appears behind the beads to form a series of streaklines. The smoke-wire is described by Corke et al. (1977). Photographs confirmed measurements made with hot-wire anemometers. These indicated that in some ranges of frequency the vortices in the shear layer would "lock in" to the forcing. Photographs also allowed the measurement of the wavelengths of the vortices and it immediately became clear that optimum effects occurred when the vortices were of comparable size to the separation bubble height (Sigurdson et al., 1981). The streaklines in the upstream stagnation region and part of the separation bubble are seen in Figure 2. This form of visualization not only indicates where the turbulent vortices are, but gives an excellent indication of the streamlines in the approximately steady potential flow region distant from the turbulence. The streaklines from the smoke-wire are associated with the streamlines if the flow is steady. Where the flow is *not* steady near the turbulence, this leads to the common novice's misinterpretation of the streaklines there to be streamlines as well. Therefore, far from the turbulence the ratio of vertical velocity v to horizontal velocity u can be calculated from the measured slope of the streaklines. This has been used to comment on the change in entrainment by the turbulent separation bubble with and without acoustic excitation (Sigurdson, 1995; Sigurdson, 1986).

Although there were indications in the smoke-wire results, it was visualization in a low-speed water channel which stimulated several ideas for the flow physics. Various

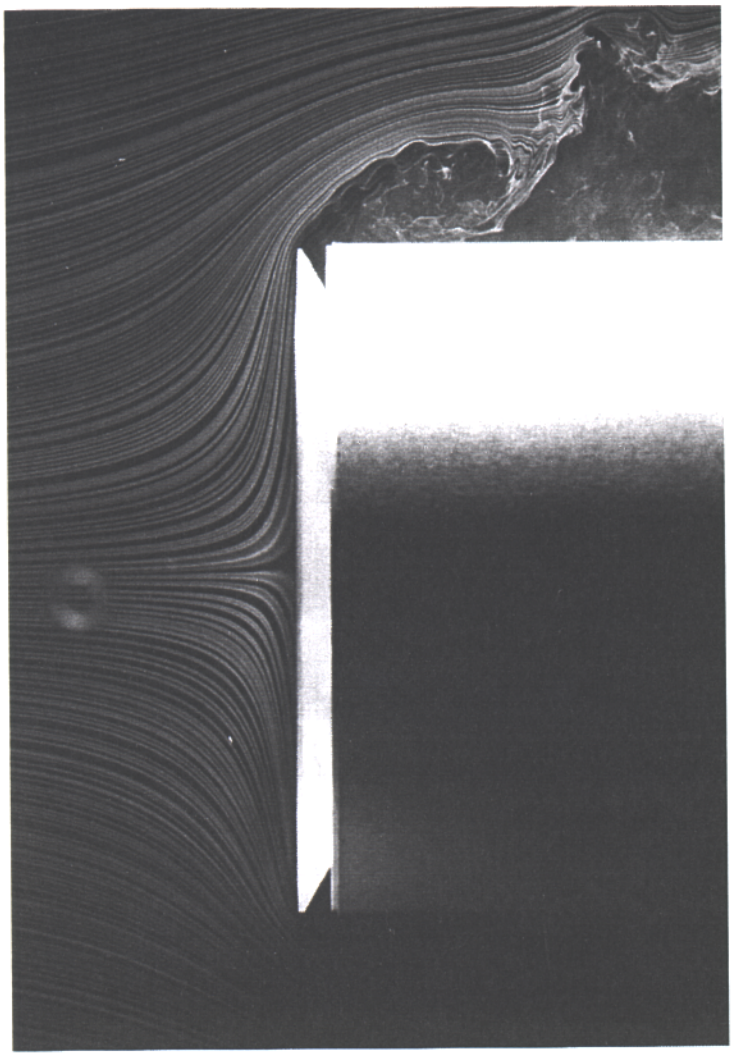

Figure 2 Streaklines impinging on the flat face of a circular cylinder aligned with the free stream. Reynolds number based on diameter is 21,200.

Lucite models were used and cobalt blue and fluorescent dye were injected in many different ways. Laser-induced fluorescence (LIF) was used to visualize a planar section of the circular cylinder flow. The argon-ion laser beam was optically processed to form a thin sheet which passed through the translucent model along a diameter. Fluorescent dye was injected from a probe upstream or from two ports located in the plane of the laser sheet diametrically opposite each other on the cylinder face. By comparing the results it was confirmed that the injection from the ports made no qualitative difference to the flow behavior, providing the injection flow rate was low enough. In all cases of injection mentioned here, the dye could be turned off and there would be enough dye resident in the recirculating region of the bubble to see that there was no noticeable effect.

Figure 3 shows one of the results for an unforced flow. The primary advantage of the LIF technique is to be able to exclude visualization of the dye which is outside the plane of the laser sheet. In this case, the vorticity of interest is primarily created on the flat face of the cylinder. If dye is placed there it will track the vorticity as discussed in the previous section. The conclusion from this photograph and others was that there are large vortical

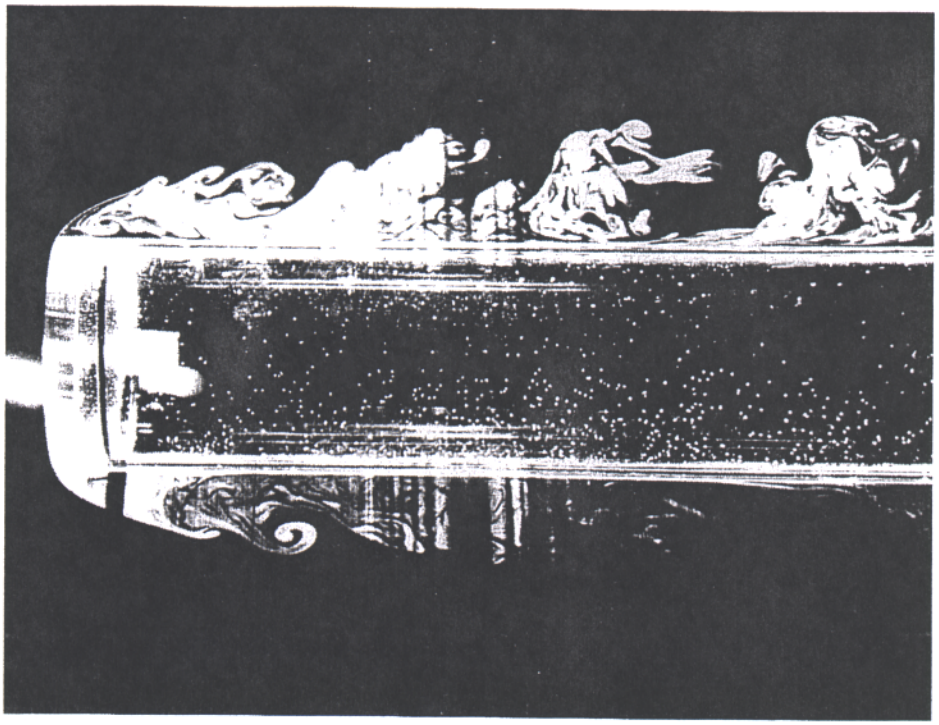

Figure 3 Laser-induced fluorescence visualization of the flow over a circular cylinder. Reynolds number based on diameter is 5150. (From Sigurdson, L.W., *JFM*, 298, 139, 1995; Sigurdson, L.W., Ph.D. thesis, Aeronautics Department, California Institute of Technology, 1986.)

structures emerging from the separation bubble and convecting downstream (Sigurdson, 1995; Sigurdson, 1986; Sigurdson and Roshko, 1985). They bore a resemblance to the well-known periodic Kármán vortices shed behind a circular cylinder aligned *transverse* to the free stream. This led to a hypothesis that there was a similarity between this "shedding" instability and Kármán vortex shedding. Now, however, the real vortices were interacting with their images due to the presence of the wall, rather than the real vortices interacting with other real vortices as in the Kármán vortex shedding case.

Further consideration resulted in a method of scaling the frequency of excitation in a manner similar to that known to be true for Kármán vortex shedding. The optimum forcing frequencies were ones which were amplified by this "shedding" type of instability. Measurements of vortex wavelength from photographs were useful in confirming these hypotheses. Estimates of the frequency could be made by using the measured wavelengths and estimated convection velocity. Video and film sequences were used for this as well. Flow visualization also played a part in validating a theory to estimate the trajectory of a free streamline which separates from the blunt face of the cylinder.

One of the things which slowed the realization of the Kármán shedding analogy was that the structures were not always so clearly apparent as in Figure 3. Further experimentation with back-lit cobalt blue dye helped explain why. The key was to introduce the dye along a slit immediately behind the sharp edge of the face of the translucent cylinder. The slit was arranged to extend along one half of the entire circumference of the cylinder. This would more comprehensively mark the vorticity and gave a three-dimensional view of the turbulence, rather than the strictly two-dimensional information from the LIF results. An example of the results is provided in Figure 4. The initial free shear layer structures are primarily two-dimensional but evolve into boundary layer-type structures as they near attachment and interact with the wall (Sigurdson and Roshko, 1984; Sigurdson, 1986).

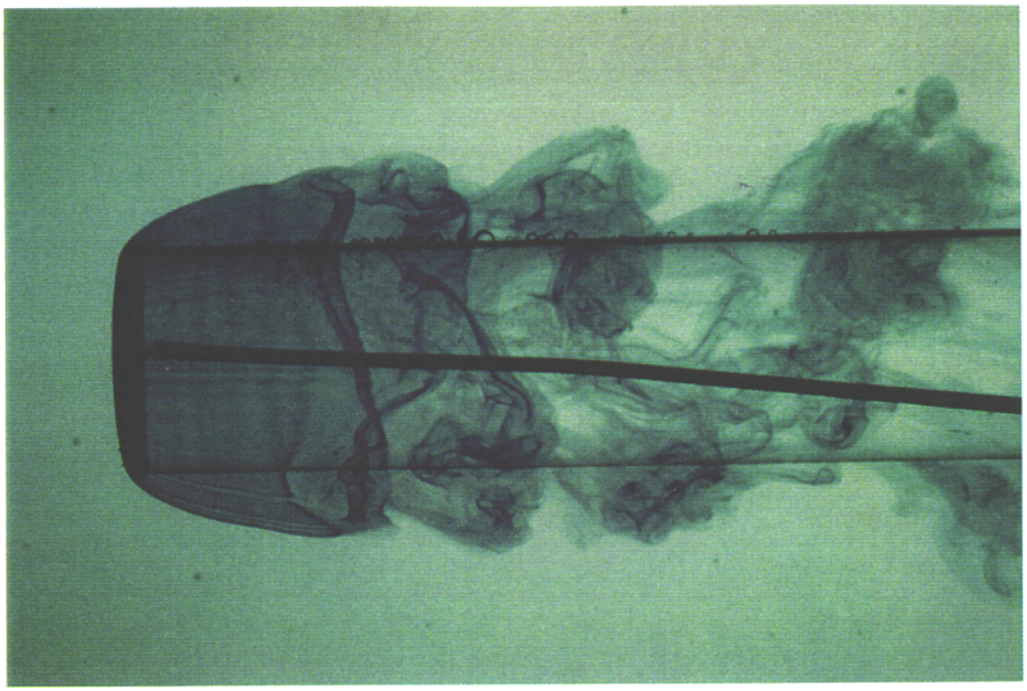

Figure 4 Cobalt blue dye injected from a slit near the leading edge of a cylinder aligned with the free stream. Reynolds number based on diameter is 2750. (From Sigurdson, L.W., Ph.D. thesis, Aeronautics Department, California Institute of Technology, 1986.)

Some segments form what roughly appear to be hairpin "loops" which convect away from the wall and downstream. Spanwise adjacent segments convect toward the wall and upstream. The loops are sometimes clearly arranged in a staggered pattern (also more recently noted by Sasaki and Kiya, 1991). A line vortex model was presented by Sigurdson (Sigurdson and Roshko, 1984; Sigurdson, 1986) that explains these observations. It was the basic three-dimensionality of the characteristic large-scale structure that complicated interpretation of the planar LIF photographs, where often the structures could not be clearly seen.

The two-dimensional counterpart of the blunt-faced cylinder, the blunt flat plate was investigated next to allow better visualization of the loop structures. Again dye was injected from a slit several plate thicknesses in length immediately behind the separation line, and at times also from a similar slit located near the reattachment region. It confirmed that the structures were qualitatively similar to those for the cylinder. Fluorescent dye was illuminated with a laser in two ways: perpendicular to both the wall and the free stream (Figure 5) and parallel to the wall (Figure 6). Figure 5 shows the characteristic "mushroom" shapes associated with the two legs of the vortex loops (the lower images are a reflecton in the plate). Figure 6 shows a staggered pattern formed by the structures as they rise away from the plate and intersect the laser sheet. Conclusions concerning the evolving topological nature of the vortex structures and their wavelengths could be drawn from photographs like these. The proposed structure reconciled apparently contradictory prepositions concerning the fate of the structures as they encounter reattachment (Sigurdson and Roshko, 1984; Sigurdson, 1986).

The nature of this flow is one of a recirculation region (separation bubble) which has, *on average*, a set of closed streamlines bounding it (Figure 1). At any *instant*, however, the three-dimensional hairpin structures were escaping the trapped orbits of the recirculation region and convecting downstream. The legs of the hairpin loop would reach upstream

Figure 5 LIF view looking upstream, sheet perpendicular to both plate and free stream, located 8.3 plate thicknesses downstream of separation. Reynolds number based on plate thickness is 890.

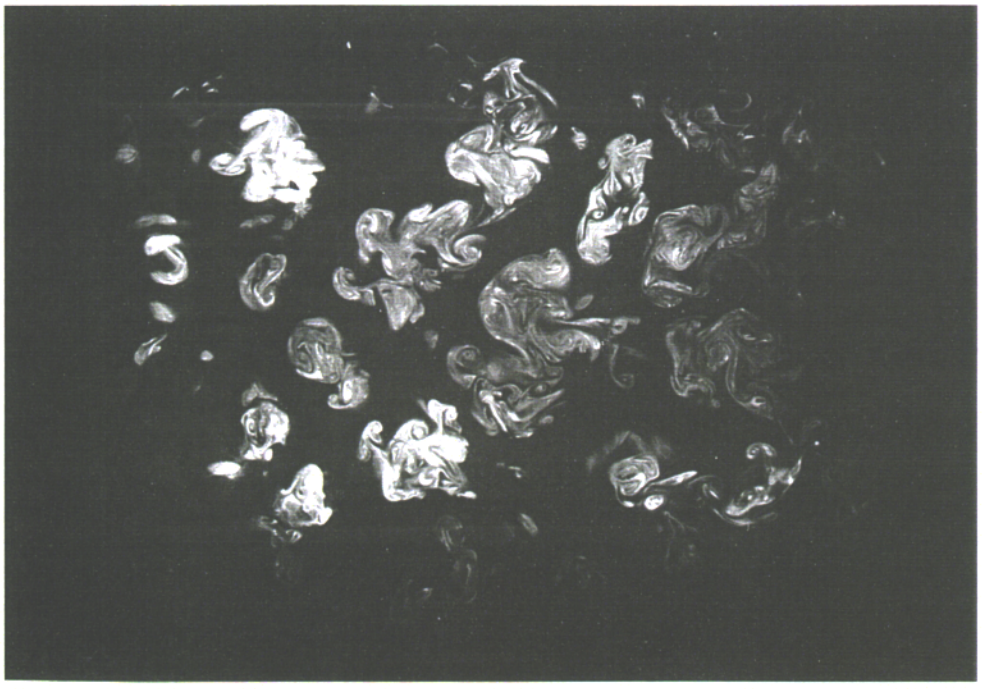

Figure 6 LIF plan view, sheet parallel to the plate, located 0.9 plate thicknesses away from the plate wall. Flow from left to right, left edge of photograph is plate leading edge. Reynolds number based on plate thickness is 850. (From Sigurdson, L.W., Ph.D. thesis, Aeronautics Department, California Institute of Technology, 1986.)

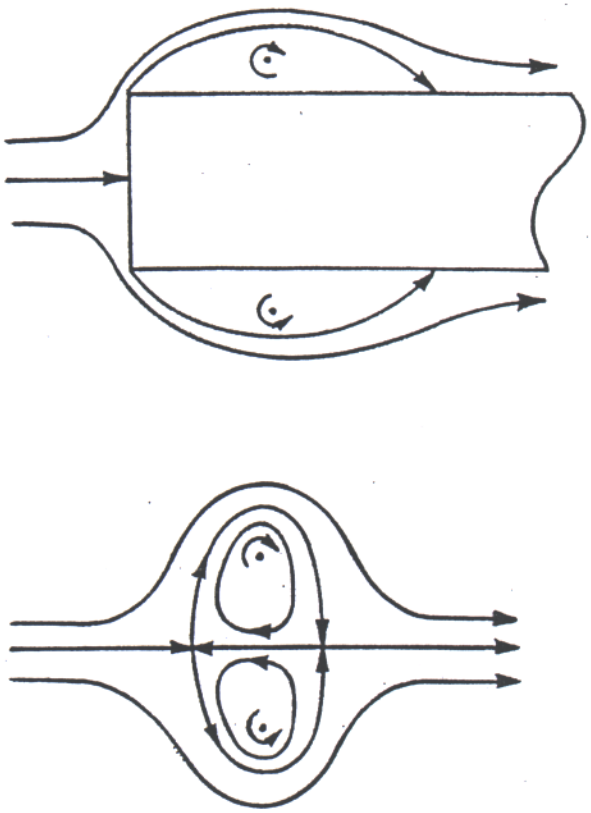

Figure 7 Comparison of the time-averaged streamlines for the cylinder or plate (top) to those for a vortex ring (bottom).

into the recirculation region and remain joined there to the adjacent loops' legs. At a later time these upstream loops would be expected to escape as well. This is explained in detail in Sigurdson (1986). The important image to hold on to now is that of the loops escaping the trapped streamlines, for it is similar to the next flows we will discuss.

Impacting Water Drops and Above-Ground Nuclear Tests

Knowledge of the three-dimensional loop structure described in the last section allowed recognition of its topologically similar existence in several other flows. Two of these are the largest-scale structure of a water drop impacting a pool of still water and the mushroom cloud from an above-ground nuclear blast. Both flows contain primary vortex rings which have similar time-averaged streamlines to the cylinder or plate flow as shown in Figure 7. The geometry of the streamlines for a vortex ring can be obtained by shrinking the cylinder to infinitesimal diameter.

First the characteristic shape of the vortex loops was seen in a bomb photograph taken by the U.S. Department of Energy in 1957, shown in Figure 8 on the right. Then aided with the knowledge that vortex tubes cannot end in the fluid (Saffman, 1992), and what kind of velocity field is implied by the presence of the vorticity through the Biot-Savart law, a hypothesized vortex skeleton structure was devised to explain the observed shapes (Sigurdson, 1987). The tracer added to the flow in this case is primarily heat and dust. The heat is from the original fireball which for this particular test (the "Priscilla" event of Operation Plumbob) was large enough to reach the ground from where the bomb was initially suspended.

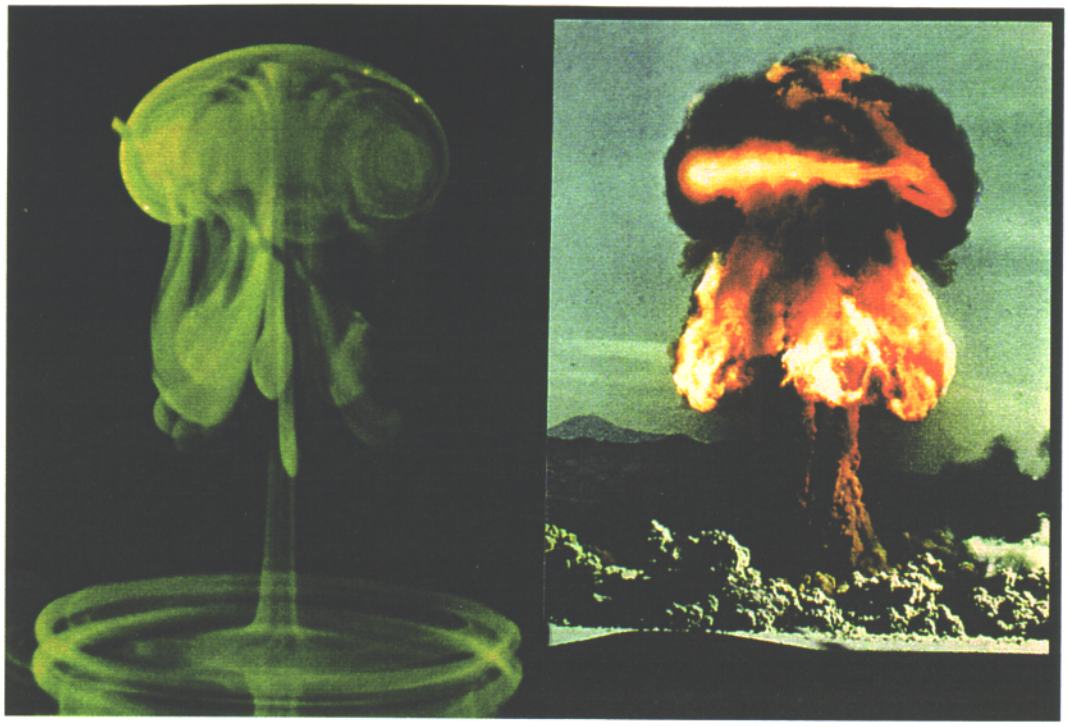

Figure 8 Comparison of the vortex structure created by a 2.6-mm water drop 50 ms after impacting a pool of water after a fall of 35 mm (inverted, left) and an above-ground nuclear test, Nevada, 1957, U.S. Department of Energy (right). (Left, from Peck, B. and Sigurdson, L.W., *Phys. Fluids*, 6[2] [Part 1], 564, 1994.)

It is conjectured that the vorticity in this problem is generated initially primarily at the interface between the hot fireball gas and the cooler surrounding air. This causes a density gradient which creates vorticity when acted on by the pressure gradients. The pressure gradients are associated with the shock wave reflected upward from the ground and the vertical hydrostatic pressure gradient from the usual resting atmosphere. This type of vorticity creation is sometimes called baroclinic torque. Since the heat tracer is not *only* initially located at the interface but throughout the fireball, the presence of heat does not in itself imply the presence of vorticity as in the previous examples. The ramifications of this to photograph interpretation concerning the water drop experiments will be discussed more fully later.

The line vortex model consists of closed line vortices in a similar fashion to the flow in the previous section: the primary ring with four azimuthal waves, four connected loops reaching to the primary ring, and four counterrotating vortex pairs forming a "stalk" which reaches from the primary ring to another ring of opposite sign situated at ground level. The topological similarity to the separation bubble is in the way the hairpin loops reach into the trapped orbits of the primary ring which are analogous to those of the separation bubble.

The detailed similarity between the water drop and the bomb was first noted by the author while looking at the drop photographs of Okabe and Inoue (1961). It seemed that the drop had a very similar basic line vortex structure to the bomb. Some results of this comparison and reasons for this similarity have been discussed previously (Sigurdson, 1987; Sigurdson, 1991), and will be the subject of another paper. Although many conclusions could be drawn from these photographs alone, more detailed information about the

drop was necessary to confirm the hypothesized structure. An experimental program was begun with Bill Peck to shed more detailed light on the structure of the impacting drop. Details are given in Peck and Sigurdson (1994) which confirm the basic hypothesized structure above and add greatly to the deeper understanding of its birth and evolution. The number of hairpin loops for the drop was observed to be three, four, or five. A photograph of the impacting drop-created vortex structure taken in our laboratory (for very specific conditions) is compared to the blast-generated vortex structure in Figure 8.

The 2.6-mm drop was dyed with fluorescent tracer and illuminated by a strobe flash 50 ms after it had fallen 35 mm and impacted the clear pool. Interruption of a laser beam by the falling drop was used to trigger a timer which controlled the time of the strobe flash after impact of the drop. Details of the careful experimental procedure necessary to create these drop photographs is given by Peck and Sigurdson (1994) and Peck et al. (1995). Various orthogonal camera angles were used to observe the structure.

Interpretation of where the vorticity is becomes more complex in this experiment because it was the *entire* drop which was originally carrying the dye, and the entire drop fluid at early times after impact is not expected to be vortical. It is expected that most of the vorticity is created at the air–water interface that is associated with the impact, therefore ideally the dye would be placed only there to track that vorticity. Consequently, on interpreting these photographs conclusions are drawn based largely on how the dye belonging to the bulk of the drop is being convected around by the vorticity. As much weight as in the cylinder or plate experiment cannot be given to the simple presence of dye as an indication of presence of vorticity. Figure 9 from Peck and Sigurdson (1991) shows a drop impacting with approximately the same conditions as in Figure 8, but at an earlier time, 9 ms after impact rather than 50 ms. This symmetric structure can evolve into the

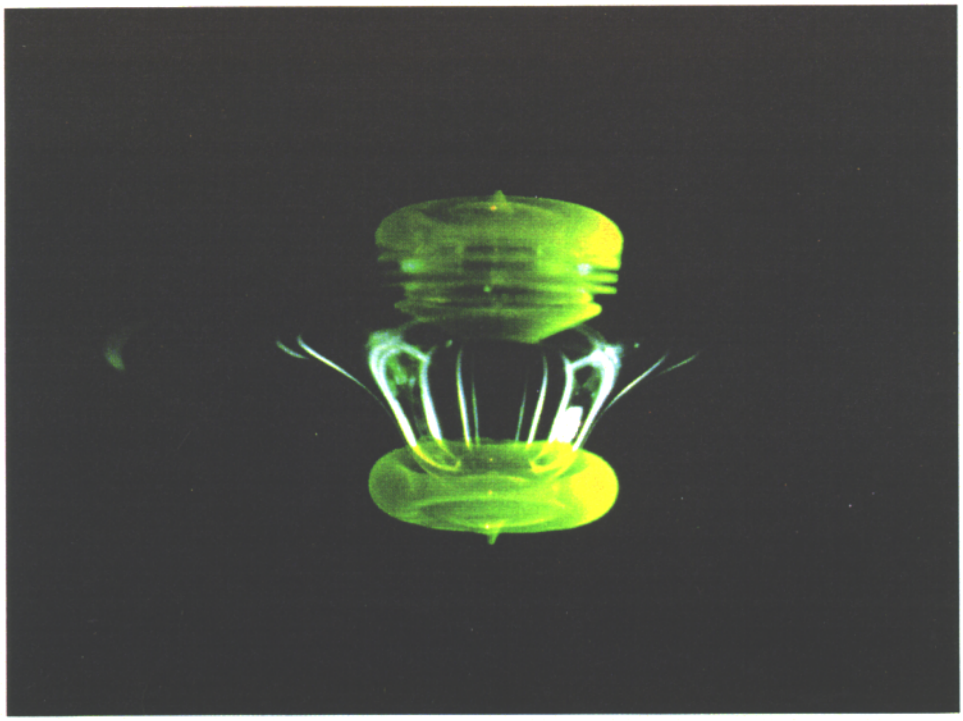

Figure 9 Structure created by a 2.8-mm water drop 9 ms after impacting a pool of clear water. It had fallen 38 mm. (From Peck, B. and Sigurdson, L.W., *Phys. Fluids*, 34[9], 2032, 1991.)

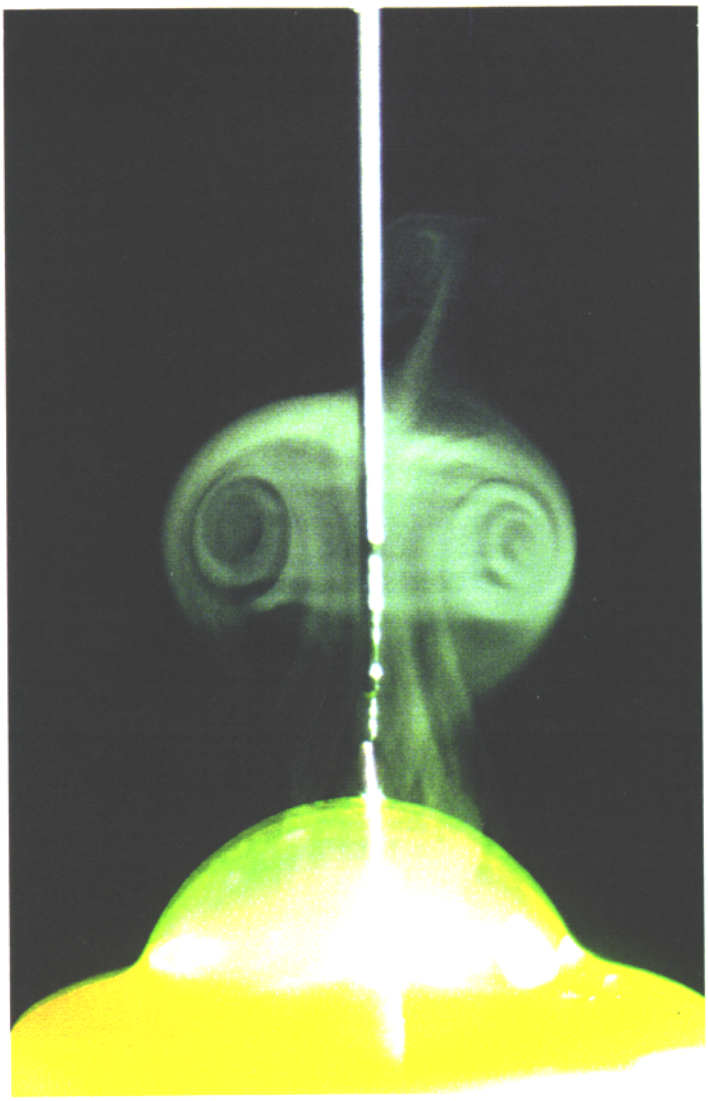

Figure 11 Triple exposure of a smoke-filled bursting air bubble showing the original bubble and resulting vortex ring. Base width of the bubble is 1.54 cm. (From Buchholz, J., Sigurdson, L.W., and Peck, B., *Phys. Fluids*, 7[9], S3, 1995.)

appreciable vorticity of opposite sign to the primary ring that is entrained into it (Sigurdson and Buchholz, 1995). Any model for vorticity creation at an air–water interface must be able to predict this and account for the fact that vortex rings are generated for both the bubble and drop despite the fact that the density and viscosity gradients across the interface are reversed in the two cases. As with the drop, velocities of the primary vortex ring can be measured using multiple-strobed photographs.

Conclusions

Four different flow types have been discussed in terms of how flow visualization has been used to elucidate the large-scale structure in each. A general methodology has been given to use for determination of the structure from interpretation of photographs obtained by

structure shown in Figure 8. The presence of vorticity is indicated by the rolling up of the dye at the edges. The photograph is taken from slightly below the water surface so a reflection of the dye is evident in the upper part. At this time the impact crater that is temporarily formed in the surface is present.

Through the use of visualization for this flow several conclusions could be drawn. Besides the structural information discussed earlier, information was learned about the transition from laminar to turbulent flow and back again (Sigurdson and Peck, 1995). Photographs recorded the shape of the oscillating drop as it falls and the capillary and larger surface waves that occur during the impact. It was found that air becomes trapped beneath the drop to sometimes form a single bubble. Velocity measurements of the resulting vortex ring could be made by making multiple exposure photographs with known time delays between strobe flashes (Peck and Sigurdson, 1995).

Bursting Air Bubbles

If a falling water drop impacting the free surface of a pool of water creates a vortex ring in the water beneath it, then one might presume the inverse of this problem would result analogously. This would be an air bubble rising in a pool of water and penetrating the free surface to create a vortex ring in the air above it, the geometry shown in Figure 10. In order to verify this and provide information about the birth and evolution of the vortex structures resulting, experiments were designed with James Buchholz to study a simpler version of the problem. It consisted of a smoke-filled air bubble resting on a free surface which was subsequently forced to break by the transmission of an electrical spark across the bubble wall. Control of the spark timing allowed photographs to be taken at various times after bubble breakage. Figure 11 from Buchholz et al. (1995a) is a triple exposure. One strobe flash exposure shows the fluorescent dyed bubble liquid before breakage. One exposure is from the flash of the spark itself, and one exposure by the strobe again shows the resulting primary vortex ring. One spark electrode can be seen coming down from the top of the bubble and another from below the bubble film. Details of the apparatus can be found in Buchholz et al. (1995b). Although researchers as far back as Rogers in 1858 (Rogers, 1858) had observed similar vortex rings, this experiment is apparently the first one to produce a photograph of the vortex ring structure.

Interpretation of the photographs is similar to the drop examples; care must be employed because the smoke tracer is originally dispersed approximately uniformly within the air bubble and not simply at the liquid–air interface where the vorticity is created. Preliminary photographs (Sigurdson et al., 1995) show that the initial roll-up of the vorticity into the primary vortex involves many smaller discrete vortex rings, a result of the Kelvin-Helmholtz instability of a free shear layer. There appear to be loops left in the wake of the primary vortex with some similarity to the drop structure, but details are still forthcoming. One result concerning the vorticity creation is that there appears to be

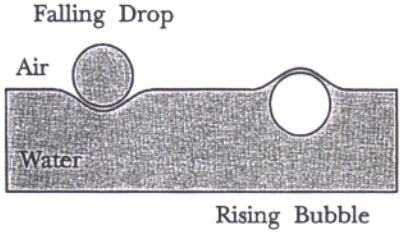

Figure 10 Schematic comparison of the falling drop and the rising bubble.

direct injection of tracer materials. Some danger areas of misinterpretation were discussed. For each flow type the basic nature of the structure was described.

Concerning the flow visualization techniques themselves, it is interesting to note how successful straightforward application of direct injection of tracers can be in providing some initial understanding of the flow behaviors. Once some idea of the nature of the structure is obtained in this way, more quantitative measurements can be much more wisely designed to characterize the flows. Although in the separated flows discussed here there was already a significant body of measurements to guide researchers, in the other examples there was not, and the contribution of the flow visualization data is quite valuable. In the separated-flows case, flow visualization offered new ideas for interpretation of previous results and resulted in useful physical insights. Some quantitative measurements of other flow features were discussed, for example, vortex ring convection velocity. When the details of the velocity field are required, elaborate methods are now available.

Concerning the nature of the flow structures observed in these examples, only a brief outline has been given. A much more in-depth consideration of the apparent similarity between the three-dimensional topology of the vortex structures discussed will be given in another paper. In these flows the topological arrangement of hairpin loops extending into the time-averaged trapped orbits of a recirculation region is a common theme. Knowledge of one led to the next. Many other flows exhibit these similarities (Sigurdson, 1986). Yet, at present, the only way to determine the structure is experimentally or through difficult (often still impossible) computation, and then careful interpretation of results using the conservation laws and knowledge of vortex dynamics. It is hoped that presenting the flow information all together in this paper may inspire other researchers to seek the equivalent of Mendeleyev's "periodic table" for turbulent structures which would aid in this process.

Acknowledgments

The work on the separated flow structure was done while I was a graduate student with Dr. Anatol Roshko and he is thanked for sharing his wisdom and support. That work was supported by the Office of Naval Research Contract N00014-76-C-0260. Some of the work on the comparison of the water drop and atomic test was supported by Darpa URI N00014-86-K-0758. The remaining work has been funded by the Natural Sciences and Engineering Research Council of Canada grant OGP0041747. Bill Peck, James Buchholz, and Bernie Faulkner are thanked for their critical roles in obtaining the drop and bubble photographs included here, among other things.

References

Buchholz, J., Sigurdson, L. W., and Peck, B., Bursting soap bubble, *Phys. Fluids*, 7(9), S3, 1995a.

Buchholz, J. H. J., Sigurdson, L. W., and Peck, B. J., An apparatus to study vortex rings emerging from bursting bubbles, in *Proc. 7th Int. Symp. Flow Vis.*, Seattle, WA, September 11–14, 1995b, 146.

Cimbala, J. M., Nagib, H. M., and Roshko, A., Large structure in the far wakes of two-dimensional bluff bodies, *JFM*, 190, 265, 1988.

Corke, T., Koga, D., Drubka, R., and Nagib, H., A new technique for introducing controlled sheets of streaklines in wind tunnels, *IEEE Publ.*, 77-CH 1251-8 AES, 1977.

Freymuth, P., On transition in a separated laminar boundary layer, *JFM*, 25(4), 683, 1966.

Kida, S. and Takaoka, M., Vortex reconnection, *Annu. Rev. Fluid Mech.*, 169, 1994.

Okabe, J. and Inoue, S., The generation of vortex rings. II, *Rep. Res. Inst. Appl. Mech. Kyushu Univ.*, 9(36), 147, 1961.

Peck, B. and Sigurdson, L. W., Impacting water drop, *Phys. Fluids*, 34(9), 2032, 1991.

Peck, B. and Sigurdson, L.W., The three-dimensional vortex structure of an impacting water drop, *Phys. Fluids*, 6(2) (Part 1), 564, 1994.

Peck, B. and Sigurdson, L. W., Vortex ring velocity resulting from an impacting water drop, *Exp. Fluids*, 18, 351, 1995.

Peck, B., Sigurdson, L. W., Faulkner, B., and Buttar, I., An apparatus to study drop-formed vortex rings, *Meas. Sci. Tech.*, 6, 1538, 1995.

Rogers, W. B., On the formulation of rotating rings by air and liquids under certain conditions of discharge, *Am. J. Sci.*, 26, 246, 1858.

Roshko, A., Structure of turbulent shear flows: a new look, *AIAA J.*, 14(10), 1349, 1976.

Saffman, P. G., Vortex interactions and coherent structures in turbulence, in *Proc. Symp. on Transition and Turbulence*, Academic Press, New York, 1980, 149.

Saffman, P. G., *Vortex Dynamics*, Cambridge Monographs on Mechanics and Applied Mathematics, Batchelor, G. K. and Freund, L. B., General Eds., Cambridge University Press, New York, 1992.

Sasaki, K. and Kiya, M., Three-dimensional vortex structure in a leading-edge separation bubble at moderate Reynolds numbers, *Trans. ASME* I: *J. Fluids Eng.*, 113, 405, 1991.

Sigurdson, L. W., (1986) The structure and control of a turbulent reattaching flow, Ph.D thesis, Aeronautics Department of California Institute of Technology, 1986.

Sigurdson, L. W., Three-dimensional vortex structure of the starting vortex ring, *Bull. Am. Phys. Soc.*, 32, 10, 1987.

Sigurdson, L. W., Atom-bomb/water drop, *Phys. Fluids A*, 3(9), 2034, 1991.

Sigurdson, L. W., The structure and control of a turbulent reattaching flow, *JFM*, 298, 139, 1995.

Sigurdson, L. W. and Buchholz, J. H., The vortex structure of impacting water drops and bursting air bubbles, *Bull. Am. Phys. Soc.*, 40(9), 1920, 1995.

Sigurdson, L. W. and Peck, B., Three-dimensional transition of the vorticity created by an impacting water drop, in *Advances in Turbulence V, Proc. 5th European Turb. Conf.*, Siena, Italy, July 5–8, 1994, Benzi, R., Ed., Kluwer Academic Publications, Dordrecht, 1995, 470.

Sigurdson, L. W. and Roshko, A., The large-scale structure of a turbulent reattaching flow, *Bull. Am. Phys. Soc.*, 29(9), 1542, 1984.

Sigurdson, L. W. and Roshko, A., A controlled unsteady excitation of a reattaching flow, *AIAA Paper*, 85-0522, 1985.

Sigurdson, L. W., Cimbala, J., and Roshko, A., Controlled excitation of a separated flow, *Bull. Am. Phys. Soc.*, 26, 9, 1981.

Sigurdson, L. W., Buchholz, J. H., and Peck, B. J., The vortex rings created by bursting air bubbles and impacting water drops, in *Proc. 15th Can. Cong. Appl. Mech. (CANCAM)*, Vol. II, University of Victoria, Victoria, BC, CA, May 28–June 2, 1995, 542.